SALÉEITE, Mg(UO₂)₂(PO₄)₂, FROM THE WOJCIESZYCE URANIUM DEPOSIT (LOWER SILESIA, POLAND)

Rafał SIUDA[1], Justyna DOMAŃSKA-SIUDA[1] & Robert BORZĘCKI[2]

[1] *Faculty of Geology University of Warsaw, Żwirki i Wigury 93, 02-089 Warszawa, Poland; siuda@uw.edu.pl*
[2] *Mineralogical Museum, Obozowa 4, 57-401 Nowa Ruda, Poland*

Abstract: The secondary uranium mineral, saléeite, was found in dumps of the former Wojcieszyce Uranium Mine. It occurs as tiny tabular crystals, up to 0.3 cm in size. The chemical formula, which was calculated on the basis of a 12 spot analyses is: $(Mg_{0.73}Fe_{0.05}K_{0.04}Ca_{0.04})_{\Sigma 0.86}(UO_2)_{2.16}(PO_4)_{2.00} \cdot 10H_2O$. The cation position is occupied mainly by Mg. The Mg ions are partially substituted by Fe, K and Ca. The tetrahedral position is occupied by the PO_4^{3-} ion. The interaction between acidic pore solutions (originating from the reaction of pyrite oxidation), uraninite and minerals of the host rocks (chlorite, apatite) leads to the release of Mg^{2+}, UO_2^{2+} and PO_4^{3-} ions. These ions are adsorbed by amorphous Fe oxyhydroxides and poorly ordered ferrihydrite. Crystallization and recrystallization of these phases leads to the release of adsorbed ions and favours the crystallization of saléeite. The coexistence of saléeite and goethite, which forms by recrystallization of ferrihydrite, points to an important role of sorption and desorption of Mg^{2+}, PO_4^{3-} and UO_2^{2+} ions in the process of crystallization of this mineral species. Crystallization of saléeite occurs at a pH of 5.5–6.0. The supergene zone of the Wojcieszyce deposit is the first occurrence of saléeite in Poland.

Key words: Saléeite, weathering of uraninite, Wojcieszyce.

Manuscript received 6 March 2015, accepted 23 May 2016

INTRODUCTION

The weathering zones of uranium deposits very often contain diverse paragenesis of secondary uranium minerals. Among these the uranyl phosphates are most common. One of group of the uranyl phosphates is the autunite group. They are characterized by low solubility; because of this they can store the uranium released during the decomposition of uraninite and other primary uranium minerals (Finch and Ewing, 1992; Murakami *et al.*, 1997; Jerden and Sinha, 2003; Gorman-Lewis *et al.*, 2008). Moreover, the immobilization of uranium from the environment can be attributed to these phases (Fuller *et al.*, 2002; Beazley *et al.*, 2009). This group includes thirteen minerals with the general formula: $A(UO_2)_2(XO_4)_2 \, 10–12H_2O$; A = Cu, Ca, Ba, Mg, Fe, Ni, X = P or As. It includes widely distributed minerals (e.g., autunite, torbernite) and minerals recorded only at a small numbers of localities (e.g., rauchite). Saléeite, which also belongs to this group, is known to occur at a number of mineralogical localities. However, the supergene zone of the Wojcieszyce deposit is the first documented occurrence of this mineral in Poland. This paper presents the results of mineralogical studies of saléeite from this locality. The authors compare their results with data from other localities. On the basis of the coexistence of saléeite with Fe-oxyhy-

droxides and data in the literature, the authors describe, in addition, the mechanism of crystallization of this mineral.

GEOLOGICAL SETTING

The Karkonosze–Izera Massif is the largest geological unit in the West Sudetes and is a part of the Bohemian Massif. The Karkonosze–Izera Massif is composed of five large units (Mazur and Aleksandrowski, 2001; Fig. 1): the Karkonosze Granite intrusion, the Izera–Kowary Unit, the Ještěd Unit, the Southern Karkonosze Unit and the Leszczyniec Unit. The central part of the Karkonosze–Izera Massif is occupied by the Variscan Karkonosze Granite. This plutonic complex subdivides the largest unit of the Karkonosze–Izera Massif, i.e. the Izera–Kowary Unit, into northern and south-eastern segments. The Izera–Kowary Unit is composed of gneisses, the Izera and Rumburk granites and mica schists. The gneisses form several regional varieties. In the northern part of the unit, the Izera orthogneisses are noteworthy, whereas in the southern and eastern parts their analogues, known as the Kowary and Karkonosze orthogneisses, occur. The gneisses are accompanied by mica schists, which are given different names in different parts of the Izera–Kowary Unit. The Złotniki Lubańskie, Stara Kamie-
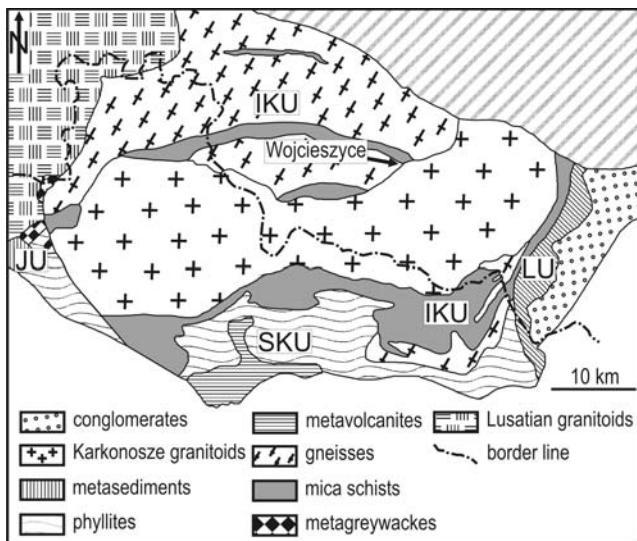
Fig. 1. Geological map of the Karkonosze-Izera massif (modified from Mazur and Aleksandrowski, 2001; Ilnicki, 2010).
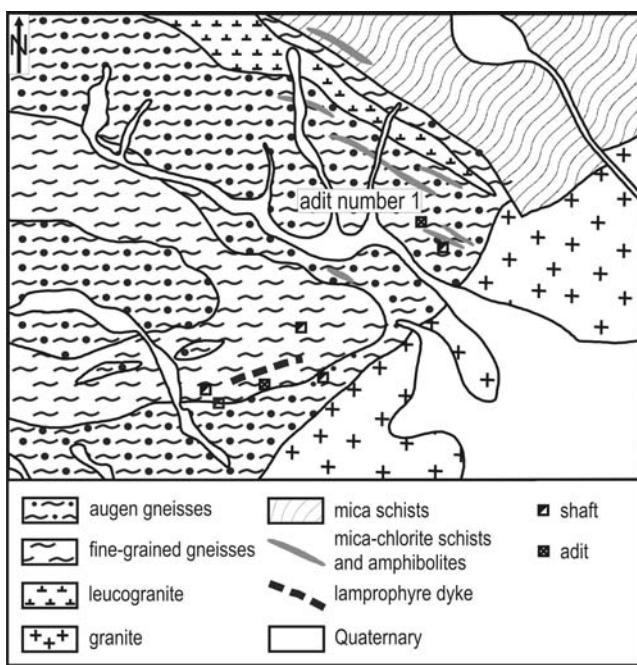
Fig. 2. Geological sketch-map of the Wojcieszyce area (*after* Szałamacha, 1965, Szałamacha, 1972, modified).

nica and the Szklarska Poręba schists crop out to the north of the Karkonosze granites.

Several small uranium deposits, which are known in the northern part of the Izera–Kowary Unit (Jaskólski, 1967; Banaś *et al.*, 1978; Mochancka and Banaś, 2000; Mochnacka *et al.*, 2015), exhibit two types of uranium mineralization. The first type is a pitchblende-fluorite mineralization of hydrothermal origin. The uranium deposit in Radionów is a typical example of such mineralization. Ore nests and veins with pitchblende, fluorite, and small amounts of pyrite and galena have been noted there (Jaskólski, 1967). The hydrothermal mineralization is overprinted by second-

ary mineralization, linked to processes of ore weathering (Jaskólski, 1967).

The second type of mineralization is dominated by secondary phases. They are accompanied by small amounts of primary hydrothermal minerals. Such mineralization occurs e.g. in the Kopaniec–Mała Kamienica area (Banaś *et al.*, 1978; Domańska-Siuda, 2010). The uranium ore at Wojcieszyce belongs to this type.

The Wojcieszyce deposit is located in the eastern part of the Izera–Kowary Unit (Fig. 2). Uranium mineralization occurs 200 to 700 m from the contact of the gneisses with the Karkonosze granite. The deposit area is composed of gneisses (coarse gneisses, fine-grained gneisses and porphyritic gneisses) locally passing into granite-gneisses and leucogranites. At the contact between the fine-grained gneisses and the porphyritic gneisses, small lenses of mica-chlorite schists and amphibolite often occur. The metamorphic rocks are cut by a lamprophyre dyke, 2 to 4 m thick, dipping from SE to NW for a distance of ca. 500 m. Numerous tectonic fissures and tectonic breccia zones oriented N–S and NW–SE occur within the metamorphic rocks.

Uranium mineralization is associated with the tectonic breccia zones and lenses of mica-chlorite schists. The dip of the mineralized zones is significant, from 50 to 80° to the north. Three ore zones have been distinguished in the deposit. The first is related to a lens of mica-chlorite schists, 1 to 4 metres thick. The schists contain zones of uranium mineralization, 0.1 to 1.5 m thick, composed of secondary uranium minerals and fine grains of uraninite (Kaczmarek, 1959). The second type of ore zone is found in tectonic fissures, 0.1 to 0.3 m wide, with autunite and uraninite accumulations. The third zone occurs at the contact between the mica-chlorite schists and the gneisses, where the mineralization includes accumulations of uraninite, accompanied by pyrite, hematite, galena and sphalerite.

The supergene zone is developed at a depth of ca. 100 m from the surface (Kaczmarek, 1959), where to date autunite and walpurgite have been recognized only on the basis of their macroscopic features, without any detailed mineralogical studies (Borucki *et al.*, 1967; Lis and Sylwestrzak, 1986). Precise age determination of the Wojcieszyce supergene mineralization is hindered by the intense Cretaceous–Palaeogene weathering processes that have affected the Karkonosze–Izera Massif area (Walczak, 1968; Migoń and Lidmar-Bergström, 2001). Parageneses of secondary uranium minerals are also found in the Karkonosze–Izera Massif area (Siuda *et al.*, 2008, 2010; Domańska-Siuda, 2010, 2012).

ANALYTICAL METHODS

Samples of secondary uranium minerals were collected from the dump of Adit No 1 of the abandoned Wojcieszyce Uranium Mine (N 50°53′19.03″, E 15°38′2.29″). XRD identification of the samples analyzed were performed using powder X-ray diffractometer X'Pert PRO MPD by the DSH method. The parameters of the X-ray beam were as follows CoKα wave length, finally monochromatized by parabolic X-rays mirror, emitted from the X-Ray tube where

40 mA and 40 kV current was applied. The X-ray pattern was recorded from the 2.5131 to 75.9891 °2Θ, with a step size of 0.02 °2Θ. The results were interpreted using X'Pert Plus HighScore (ver. 2.2e) software and a ICDD PDF-2 database (Release 2008 RDB).

Chemical analyses of saléeite were carried out, using a Cameca SX-100 electron microprobe at the Inter-Institute Analytical Complex for Minerals and Synthetic Substances, University of Warsaw. In order to minimize peak overlapping, the following analytic lines, crystals and standards were selected: V (Kα, LIF, V_2O_5), Mn (Kα, LIF, rhodochrosite), Fe (Kα LIF, Fe_2O_3), Cu (Kα LIF, chalcopyrite), Zn (Kα LIF, ZnS), Ba (Lα LIF, barite), Na (Kα TAP, albite), Mg (Kα TAP, diopside), Al (Kα TAP, orthoclase), Si (Kα TAP, diopside), As (Lα TAP, GaAs), U (Mα PET, UO_2), Pb (Mα PET PbCrO₄), Bi (Mα PET, Bi_2Se_3), P (Kα PET, apatite), K (Kα PET, orthoclase), Ca (Kα PET, diopside). Analyses were conducted at an accelerating voltage of 15 kV and beam current of 10 nA. The beam diameter was 10–20 μm. ZAF corrections were used. Elevated analytical totals of saléeite are caused by water evaporation in high vacuum or heating of the analyzed spot by the electron beam.

IR absorption spectra were recorded with a *Nicolet Magna 550* spectrometer from 4000 to 400 cm^{-1}, using KBr pellets (Faculty of Chemistry, Warsaw University).

RESULTS

The Wojcieszyce saléeite occurs as fine, up to 0.3 cm, tabular translucent crystals (Fig. 3). The crystals form coatings of up to 3 cm² on the surfaces of biotite-chlorite schists. In some cases, they occur as comb-like aggregates of tabular crystals growing on the walls of small voids, resulting from the leaching of pyrite aggregates. Occasionally, the aggregates of crystals completely fill up the voids (Fig. 4A). Saléeite is always accompanied by older, brown goethite (Fig. 4B).

Fig. 3. Tabular crystals of saléeite (bright crystals) growing on goethite (gt).

The presence of saléeite was confirmed by the PXRD method. The X-ray powder diffraction pattern of the studied saléeite (Table 1) corresponds to data published for this mineral (Plášil *et al.*, 2009). The X-ray diffraction of saléeite indicates metatorbernite traces ($d_{0.002}$ 8.698 Å) only. The presence of meta-saléeite, which is the phase formed during the dehydration of saléeite, was not observed. The refined unit-cell parameters of saléeite from Wojcieszyce are: a = 5.1741 [Å], b = 19.5717 [Å], c = 10.2233 [Å], β = 104.086 [°], V = 1004.13 [Å³]. These values are typical for the saléeite (*see* Plášil *et al.*, 2009), with the exception of the a parameter, which is reduced.

The chemical composition of saléeite from Wojcieszyce is given in Table 2. The elevated analytic total of saléeite is generally caused by water evaporation under high vacuum conditions and heating of the analyzed spots by the electron beam.

At the cation sites the dominant element is Mg, whose content varies within 0.60 to 0.93 a.p.f.u. This element is accompanied by iron (up to 0.17 a.p.f.u.), potassium (from
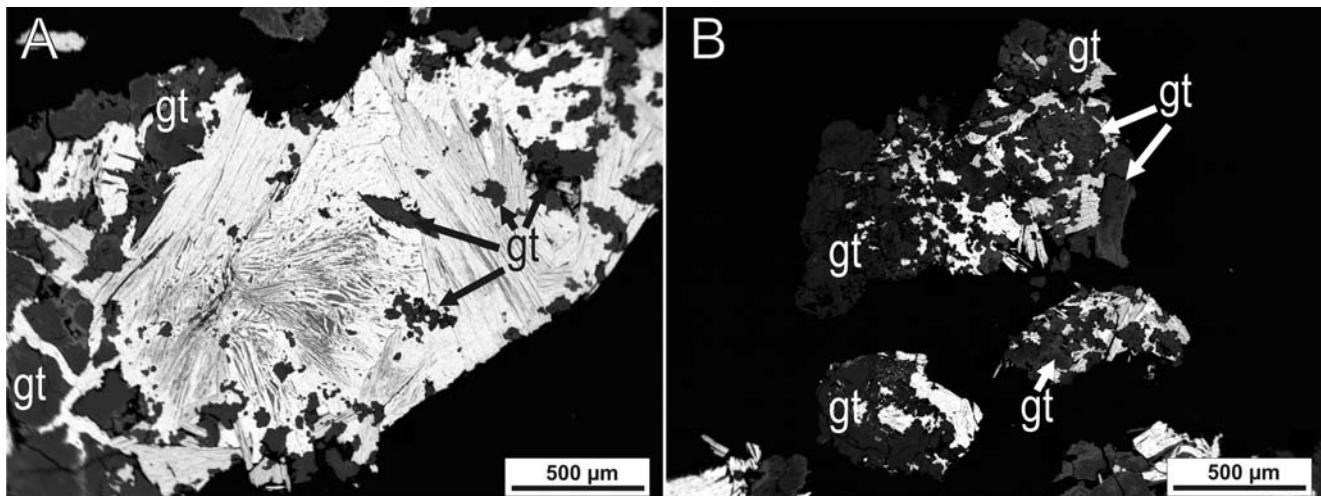
Fig. 4. BSE images of aggregates of saléeite filling void after pyrite (**A**) and aggregates of saléeite and goethite filling cavities after pyrite (**B**).

Table 1

X-ray powder diffraction pattern of saléeite from Wojcieszyce

h	k	l	d_{obs}	d_{calc}	I_{rel}
1	0	0	9.955	9.957	100
2	0	0	4.965	4.967	35
0	4	0	4.904	4.903	6
0	3	1	3.475	3.473	9
2	5	-1	3.084	3.084	1
1	5	1	2.462	2.462	5
1	8	-1	2.201	2.200	1
3	5	-2	2.160	2.154	2
2	5	1	2.101	2.105	5
2	9	-1	1.994	1.995	12
2	7	1	1.863	1.862	3
4	7	0	1.854	1.855	2
3	9	0	1.818	1.817	2
4	8	0	1.741	1.742	1
0	6	2	1.735	1.735	1
4	10	-1	1.661	1.660	4
0	11	1	1.632	1.632	3

0.03 to 0.06 a.p.f.u.), calcium (from 0.02 to 0.07 a.p.f.u.) and copper (up to 0.01 a.p.f.u.). Replacement of Mg^{2+} ions by Ca^{2+} and K^+ ions observed in the mineral analyzed indicates that the mineral belong to different isomorphic series such as saléeite-autunite ($Ca(UO_2)_2(PO_4)_2 \cdot 10$–$12H_2O$) and saléeite-meta-ankoleite ($K_2(UO_2)_2(PO_4)_2 \cdot 6H_2O$) (Fig. 5A). It is thus most similar to the saléeite, described from Medvědín (Plášil *et al.*, 2009) and Vale de Abrutiga (Cabral Pinto *et al.*, 2008). On the other hand, intensive substitution of Mg^{2+} ions by ions with a smaller ionic radius (mainly Fe^{2+}) observed at the cation sites may indicate that the saléeite from Wojcieszyce belongs to the saléeite-bassetite ($Fe^{2+}(UO_2)_2(PO_4)_2 \cdot 8H_2O$) isomorphic series (Fig. 5B). Saléeite enriched in Fe has been described e.g. from Vale de Abrutiga (Cabral Pinto *et al.*, 2008) and from the Eduardo Mine (Yakubovich *et al.*, 2008).

The tetrahedral site is occupied by the PO_4^{3-} anion only. In relation to the content of the phosphate ion, the saléeite from Wojcieszyce is similar to the saléeite from Arcu su Linnarbu (Vochten and van Springel, 1996), Kladská (Pauliš *et al.*, 1999), Sabugal (Frondel, 1951) and Shinkolobwe (Thoreau and Vaes, 1932).

The following empirical formula was calculated from the average of 12 spot analyses on the basis of P = 2 is $(Mg_{0.73}Fe_{0.05}K_{0.04}Ca_{0.04})_{\Sigma0.86}(UO_2)_{2.16}(PO_4)_{2.00} \cdot 10H_2O$.

Infrared spectrum of saléeite (Fig. 6) presents readily visible the vibration modes of the tetrahedral PO_4^{3-} group: ν_4 O-P-O bending (550 cm^{-1}), ν_3 P-O stretching (1009 cm^{-1},

Table 2

Chemical composition of saléeite from Wojcieszyce

wt %	Analysis											
	1	2	3	4	5	6	7	8	9	10	11	12
MgO	4.38	3.73	3.70	3.83	3.75	3.98	3.23	3.03	3.33	2.99	2.92	3.13
K₂O	0.28	0.31	0.16	0.27	0.21	0.16	0.31	0.16	0.28	0.16	0.27	0.21
CaO	0.28	0.42	0.21	0.29	0.14	0.21	0.23	0.19	0.33	0.16	0.47	0.27
FeO	0.00	0.00	0.00	0.00	0.00	1.47	0.60	0.77	0.51	0.52	0.59	0.68
CuO	0.00	0.00	0.00	0.00	0.00	0.00	0.00	0.00	0.14	0.00	0.00	0.13
P₂O₅	16.65	18.32	17.45	17.32	16.84	16.67	15.11	15.28	17.13	16.06	17.05	17.77
UO₃	68.51	73.34	73.17	74.03	70.65	69.62	73.50	73.84	74.19	74.66	75.19	74.04
H₂O*	21.13	23.25	22.15	21.98	21.38	21.16	19.18	19.39	21.74	20.39	21.64	22.55
Total	111.22	119.36	116.84	117.71	112.97	113.27	112.16	112.65	117.64	114.95	118.11	118.76
a.p.f.u.												
Mg	0.93	0.72	0.75	0.78	0.78	0.84	0.75	0.70	0.68	0.66	0.60	0.62
K	0.05	0.05	0.03	0.05	0.04	0.03	0.06	0.03	0.05	0.03	0.05	0.03
Ca	0.04	0.06	0.03	0.04	0.02	0.03	0.04	0.03	0.05	0.03	0.07	0.04
Fe	0.00	0.00	0.00	0.00	0.00	0.17	0.08	0.10	0.06	0.06	0.07	0.08
Cu	0.00	0.00	0.00	0.00	0.00	0.00	0.00	0.00	0.01	0.00	0.00	0.01
Σ cations	1.02	0.83	0.80	0.87	0.84	1.08	0.93	0.86	0.86	0.78	0.79	0.78
P	2.00	2.00	2.00	2.00	2.00	2.00	2.00	2.00	2.00	2.00	2.00	2.00
Σ anions	2.00	2.00	2.00	2.00	2.00	2.00	2.00	2.00	2.00	2.00	2.00	2.00
U	2.04	1.99	2.08	2.12	2.08	2.07	2.41	2.40	2.15	2.31	2.19	2.07
H₂O	10.00	10.00	10.00	10.00	10.00	10.00	10.00	10.00	10.00	10.00	10.00	10.00

H₂O* – content of H₂O was calculated on the basis of 10 H₂O molecules in ideal saléeite formula
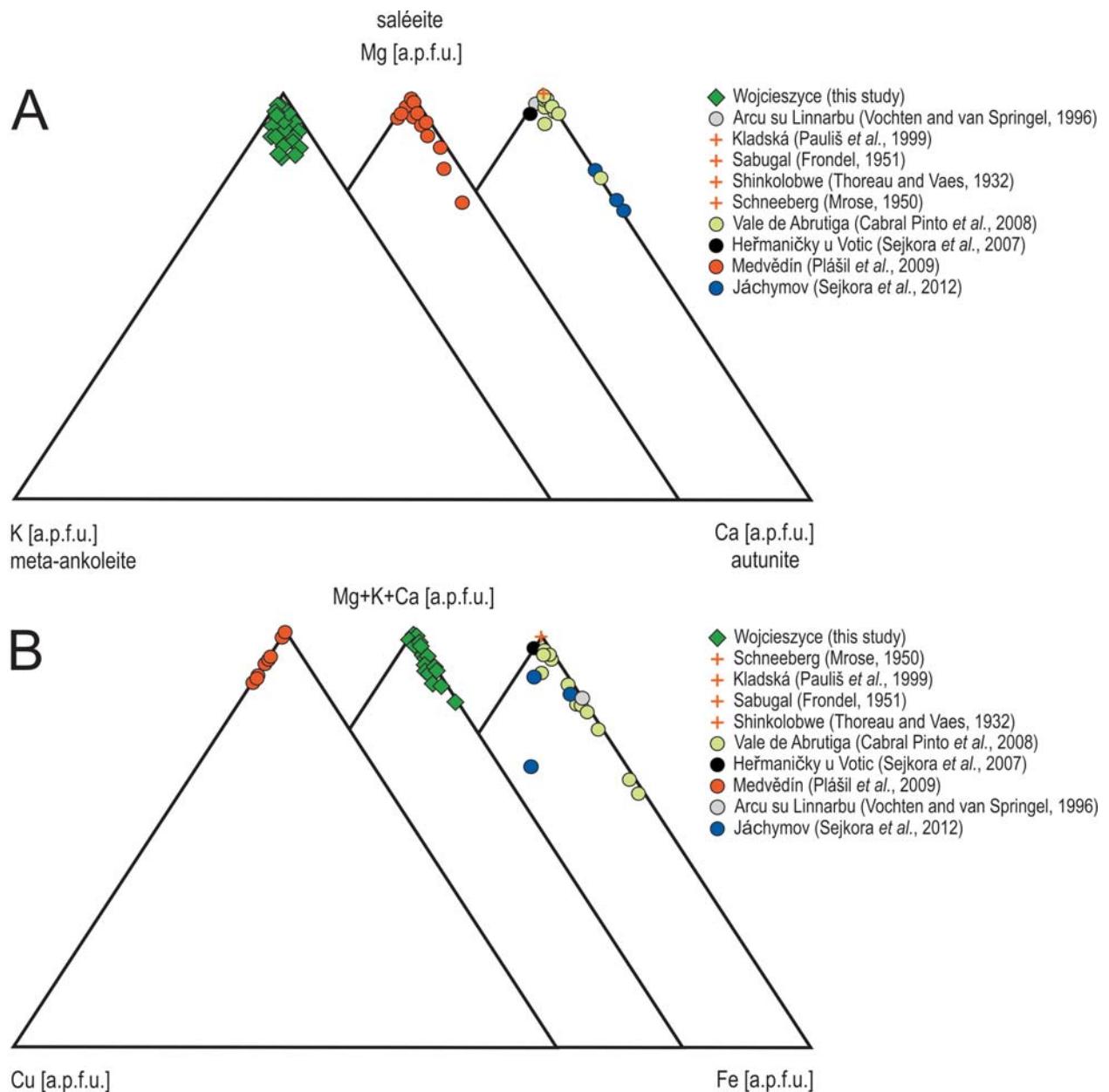
Fig. 5. Ternary plot of chemical composition of saléeite from Wojcieszyce (in atoms per formula unit). **A.** Occupancy of anionic position in Mg-K-Ca system. **B.** Occupancy of anionic position in (Mg+K+Ca)-Cu-Fe system.

1114 cm^{-1}). The absorption bands at 3403, 3217 cm^{-1} (shoulder) are connected with stretching vibrations of H-O bond. The band at 1642 cm^{-1} corresponds to bending vibrations of H-O-H bonds in water molecules. A weakly visible band at 620 cm^{-1} is probably connected with the liberation modes of water molecules. A weak absorption band at 847 cm^{-1} is assigned to the symmetric stretching vibration ν_1 UO$_2^{2+}$. A sharp absorption band at 917 cm^{-1} is assigned to the antisymmetric stretching vibration ν_3 UO$_2^{2+}$. The recorded infrared spectrum of the saléeite from Wojcieszyce is very similar to that of the ferrous saléeite from Arcu su Linnarbu (Vochten and van Springel, 1996). The absence of absorption bands connected with the presence of AsO$_4^{3-}$ and other anions confirm the results of the chemical analyses.

ORIGIN OF SALÉEITE

The supergene zone of the Wojcieszyce uranium deposit is developed at a depth of ca. 100 metres from the surface. Particular intensification of the supergene processes and the presence of secondary uranium minerals can be observed along the fault planes containing primary ore mineralization, composed of pyrite, uraninite, galena and sphalerite. Faults favoured the migration of groundwater that affected the ore minerals and minerals, occurring in the rocks surrounding the deposit. The formation of saléeite is linked with multistage processes taking place in the supergene zone, including the decomposition of primary hydrothermal mineralization and barren minerals, sorption of ions on the
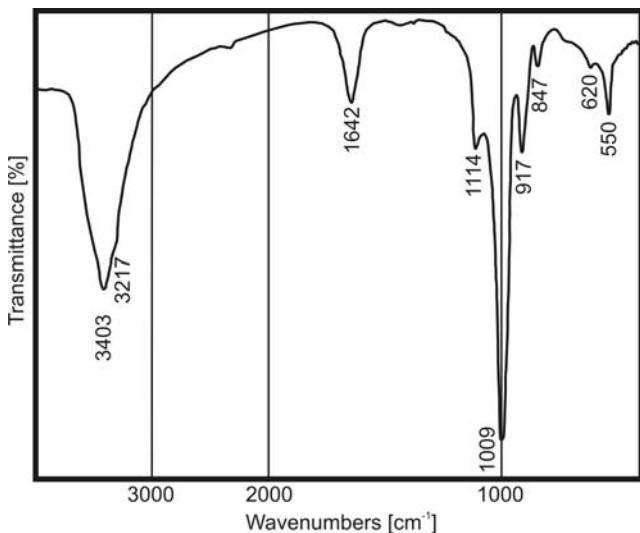
Fig. 6. Infrared spectrum of saléeite from Wojcieszyce.

released iron oxyhydroxides and crystallization of uranyl phosphates at the surfaces of these phases.

Pyrite occurring in the deposit undergoes oxidation in the presence of oxygen-enriched meteoric waters, migrating downwards into the deposit. One of the products of this reaction is Fe^{2+} ions, which can be oxidized to Fe^{3+} ions. The Fe^{3+} ion is characterized by very strong oxidative potential, causing much faster pyrite decomposition, which results in a drastic drop of pH within the environment *via* the formation of chemically aggressive acidic solutions. In the supergene zone, uraninite is a mineral that rather easily undergoes oxidation in the presence of atmospheric oxygen or oxygen dissolved in groundwater. Its oxidation is accelerated by the effect caused by Fe^{3+} ions (Deditius *et al.*, 2007). They cause oxidation of U^{4+} to U^{6+}, which occurs in the form of the uranyl ion that is readily soluble in water with respect to U^{4+} (e.g., Langmuir, 1978). The alteration of uraninite is accelerated under low pH conditions (Pérez del Villar *et al.*, 2002). Chemically aggressive groundwaters with low pH also have an effect on rock-forming minerals in the surrounding rocks, e.g. chlorite present in the mica-chlorite schists. At low pH, this mineral undergoes decomposition and releases significant amounts of Mg^{2+} ions into the groundwater (Parafiniuk, 1996). Acidic solutions generated during pyrite oxidation also influence the accessory apatite occurring in the gneisses. At low pH, this mineral is dissolved (Pérez del Villar *et al.*, 2002), becoming a source of orthophosphate ions. Their concentration in the solution, at which crystallization of uranyl phosphates is possible, should be around 10^{-2} mol/kg (Markovic and Pavkovic, 1983; Sandino and Bruno, 1992). As the accessory apatite is present in only low amounts, reaching a relevant concentration of phosphate ions (following the dissolution of apatite) in the supergene zone studied is highly improbable. However, these ions can locally increase in the solution as a result of desorption process of Fe-oxyhydroxides.

Intensified precipitation of Fe-oxyhydroxides (mainly ferrihydrite) is caused by an increase in the pH of the ground-

water. Fe-oxyhydroxides strongly adsorb uranyl ions (e.g., Waite *et al.*, 1994; Moyes *et al.*, 2000; Neiva *et al.*, 2014) and phosphate ions. On the other hand, ferrihydrite is thermodynamically unstable and transforms into goethite. Goethite, formed during the recrystallization of ferrihydrite, is characterized by much lower sorption properties. This causes the release of earlier adsorbed UO_2^{2+} and PO_4^{3-} ions and a local increase in their concentration within the recrystallizing aggregates of Fe-oxyhydroxides (Payne and Airey, 2006; Cabral Pinto *et al.*, 2014). The UO_2^{2+} and PO_4^{3-} ions released react with Mg^{2+} ions present in solution favouring the crystallization of saléeite, crystals of which are always linked with goethite accumulations replacing the weathering ion sulphides (Fig. 4B). An analogous mechanism of growth of this mineral was also observed e.g. in the Koongarra deposit in Australia (Murakami *et al.*, 1997, 2005) and in the supergene zone of the uranium deposit at Vale de Abrutiga (Cabral Pinto *et al.*, 2014). A similar crystallization mechanism was also observed for other phosphates from the autunite group (Sato *et al.*, 1997).

Geochemical modelling for the supergene zone of the uranium deposit in Bangombé (Jensen *et al.*, 2002) indicates that the saléeite analyzed crystallizes in the presence of weakly acidic solutions, with a pH not exceeding 5.5–6. These pH values were confirmed also by Göb *et al.* (2013). Similar pH values are also indicated by the presence of ferrihydrite. This mineral precipitates from waters with a pH above 5.5 (Murad and Roík, 2003).

CONCLUSIONS

The saléeite studied is a product of the alteration of primary uranium mineralization. The analyzed mineral is characterized by a homogeneous chemical composition, displaying only minor substitutions of the Mg^{2+} ion by Fe^{2+}, K^+ and Ca^{2+}. The saleeite from Wojcieszyce is a magnesium-rich member of the saléeite-autunite and saléeite-meta-ankoleite isomorphic series. The tetrahedral site is occupied by the PO_4^{3-} anion only.

The crystallization of saléeite is a multistep process that begins with the decomposition of uraninite, chlorite and apatite. The uranyl and phosphate ions released are adsorbed by Fe-oxyhydroxide aggregates, generated by pyrite oxidation. Recrystallization of Fe-oxyhydroxides leads to the formation of goethite and the liberation of adsorbed ions, which react with Mg^{2+} ions present in solution and the saléeite crystallized within goethite accumulations. The formation of saléeite occurs, where the pH values are in the range 5.5–6.0. The weathering zone of the Wojcieszyce uranium deposit is the first documented occurrence of saléeite in Poland.

comments. Special thanks go to Geoffrey Manby for improving the English text.

REFERENCES

Banaś, M., Jaskólski, S., Mochnacka, K. & Salamon, W., 1978. Przejawy mineralizacji uranowej w rejonie Pasma Kamienickiego (Pogórze Izerskie). *Zeszyty Naukowe Akademii Górniczo-Hutniczej, Geologia*, 2: 105–165. [In Polish.]

Beazley, M., Martinem, R., Sobecky, P., Webb, S. & Taillefert, M., 2009. Nonreductive biomineralization of uranium (VI) phosphate via microbial phosphatase activity in anaerobic conditions. *Geomicrobiology Journal*, 26: 431–441.

Borucki, J., Głowacki, Z., Masłowski, W., Sałdan, M., Uberna, J. & Zajączkowski, W., 1967. Ocena perspektyw poszukiwawczych złóż rud uranu w Polsce. *Prace Państwowego Instytutu Geologicznego*. Warszawa. 1–93. [In Polish.]

Cabral Pinto, M. M. S., Silva, M. M. V. G. & Neiva, A. M. R., 2008. Geochemistry of U-bearing minerals from the Vale de Abrutiga uranium mine area, Central Portugal. *Neues Jahrbuch für Mineralogie Abhandlungen*, 185: 183–198.

Cabral Pinto, M. M. S., Silva, M. M. V. G. & Neiva, A. M. R., 2014. Release, migration, sorption and (re)precipitation of U during a granite alteration under oxidizing conditions. *Procedia Earth and Planetary Science*, 8: 28–32.

Deditius, A. P., Utsunomiya, S. & Ewing, R. C., 2007. Fate of trace elements during alternation of uraninite in a hydrothermal vein-type U-deposit from Marshall Pass, Colorado, USA. *Geochimica et Cosmochimica Acta*, 71: 4954–4973.

Domańska-Siuda, J., 2010. New data on secondary uranium minerals from the Western Sudetes (Poland) – preliminary report. *Mineralogia Special Papers*, 37: 106.

Domańska-Siuda, J., 2012. Brannerite and associated uranium minerals from Wołowa Góra (Karkonosze Mts., Poland). *Biuletyn Państwowego Instytutu Geologicznego*, 449: 393–399. [In Polish, with English summary.]

Finch, R. J. & Ewing, R. C., 1992. The corrosion of uraninite under oxidizing conditions. *Journal of Nuclear Materials*, 190: 133–156.

Frondel, C., 1951. Studies of uranium minerals (IX); Saléeite and novacekite. *American Mineralogist*, 36: 680–686.

Fuller, C. C., Bargar, J. R., Davis, J. A. & Piana, M. J., 2002. Mechanisms of uranium interactions with hydroxyapatite: implications for groundwater remediation. *Environmental Science and Technology*, 36: 4642–4649.

Gorman-Lewis, D., Burns, P. C. & Fein, J. B., 2008. Review of uranyl mineral solubility measurements. *Journal of the Chemical Thermodynamics*, 40: 335–352.

Göb, S., Gührig, J. E., Bau, M. & Markl, G., 2013. Remobilization of U and REE and the formation of secondary minerals in oxidized U deposits. *American Mineralogist*, 98: 530–548.

Ilnicki, S., 2010. Petrogenesis of continental mafic dykes from the Izera Complex, Karkonosze-Izera Block (West Sudetes, SW Poland). *International Journal of Earth Sciences*, 99: 745–773.

Jaskólski, S., 1967. Polymetallic oxide-sulfide mineralization in granitic gneisses of the Izera Mts. (Lower Silesia) and its genesis. *Prace Geologiczne Polskiej Akademii Nauk*, 43: 7–78. [In Polish, with English summary.]

Jensen, K. A., Palenik, C. S. & Ewing, R. C., 2002. U^{6+} phases in the weathering zone of the Bangombé U-deposit: observed and predicted mineralogy. *Radiochimica Acta*, 90: 761–769.

Jerden, J. L. & Sinha, A. K., 2003. Phosphate based immobilization of uranium in an oxidizing bedrock aquifer. *Applied Geochemistry*, 18: 823–843.

Kaczmarek, J., 1959. Ocena uranonośności Sudetów w oparciu o wyniki dotychczasowych prac poszukiwawczych prowadzonych przez Zakłady Przemysłowe R1. *Materiały faktyczne – paszportyzacja złóż i punktów okruszcowania, tom II.* Praca zbiorowa, Kowary 1959 (typescript), Państwowe Archiwum we Wrocławiu. [In Polish.]

Langmuir, D., 1978. Uranium solution-mineral equilibria at low temperatures with applications to sedimentary ore deposits. *Geochimica Cosmochimica Acta*, 42: 547–569.

Lis, J. & Sylwestrzak, H., 1986. *Minerały Dolnego Śląska*. Wydaw-nictwa Geologiczne, Warszawa, 791 pp. [In Polish.]

Markovic, M. & Pavkovic, N., 1983. Solubility and equilibrium constants of uranyl(2+) in phosphate solutions. *Inorganic Chemistry*, 22: 978–982.

Mazur, S. & Aleksandrowski, P., 2001. The Tepla(?)/Saxothuringian suture in the Karkonosze-Izera massif, western Sudetes, central European Variscides. *International Journal of Earth Sciences (Geologische Rundschau)*, 90: 341–360.

Migoń, P. & Lidmar-Bergström, K., 2001. Weathering mantles and their significance for geomorphological evolution of central and northern Europe since the Mesozoic. *Earth Science Reviews*, 56: 285–324.

Mochnacka, K. & Banaś, M., 2000. Occurrence and genetic relationship of uranium and thorium mineralization in the Karkonosze–Izera Block (the Sudety Mts, SW Poland). *Annales Societatis Geologorum Poloniae*, 70: 137–150.

Mochancka, K., Oberc-Dziedzic, T., Mayer, W. & Pieczka, A., 2015. Ore mineralization related to geological evolution of the Karkonosze-Izera Massif (the Sudetes, Poland) – Towards a model. *Ore Geology Reviews*, 64: 215–238.

Moyes, L. N., Parkman, R. H., Charnock, J. M., Vaughan, D. J., Livens, F. R., Hughes, C. R. & Braithwaite, A., 2000. Uranium uptake from aqueous solution by interaction with goethite, lepidocrocite, muscovite and mackinawite: an X-ray absorption spectroscopy study. *Environmental Science and Technology*, 34: 1062–1068.

Mrose, M. E., 1950. Studies of uranium minerals (III): saléeite from Schneeberg, Saxony. *American Mineralogist*, 35: 525–530.

Murad, E. & Roík, P., 2003: Iron-rich precipitates in a mine drainage environment: Influence of pH on mineralogy. *American Mineralogist*, 88: 1915–1918.

Murakami, T., Ohnuki, T., Isobe, H. & Sato, T., 1997. Mobility of uranium during weathering. *American Mineralogist*, 82: 888–899.

Murakami, T., Sato, T., Ohnuki, T. & Isobe, H., 2005. Field evidence for uranium nanocrystallization and its implications for uranium transport. *Chemical Geology*, 221: 117–126.

Neiva, A. M. R., Carvalho, P. C. S., Antunes, I. M. H. R., Silva, M. M. V. G., Santos, A. C. T., Cabral Pinto, M. M. S. & Cunha, P. P., 2014. Contaminated water, stream sediments and soils close to the abandoned Pinhal do Souto uranium mine, central Portugal. *Journal of Geochemical Exploration*, 136: 102–117.

Parafiniuk, J., 1996. Sulfate minerals and their origin in the weathering zone of the pyrite-bearing schists at Wieściszowice (Rudawy Janowickie Mts, Western Sudetes). *Acta Geologica Polonica*, 46: 353–414.

Pauliš, P., Ševců, J., Novotný, J. & Rendl, J., 1999. Saléeit a minerál izomorfní řady fosfuranylit-yingjiangitové z uranového ložiska Kladská u Mariánských Lázní. *Věstník Českého Geologického Ústavu*, 74: 47–49. [In Czech, with English summary.]

Payne, T. E. & Airey, P. L., 2006. Radionuclide migration at the

Koongarra uranium deposit, Northern Australia – Lessons from the Alligator Rivers analogue project. *Physics and Chemistry of the Earth*, 31: 572–586.

Pérez del Villar, L., Bruno, J., Campos, R., Gómez, P., Cózar, J. S., Garralón, A., Buil, B., Arcos, D., Carretero, G., Ruiz Sánchez-Porro, J. & Hernán, P., 2002. The uranium ore from Mina Fe (Salamanca, Spain) as a natural analogue of processes in a spent fuel repository. *Chemical Geology*, 190: 395–415.

Plášil, J., Sejkora, J., Čejka, J., Škoda, R. & Goliáš, V., 2009. Supergene mineralization of the Medvědín uranium deposit, Krkonoše Mountains, Czech Republic. *Journal of Geosciences*, 54: 15–56.

Sandino, A. & Bruno, J., 1992. The solubility of $(UO_2)_3(PO_4)_2 \cdot 4H_2O_{(s)}$ and the formation of U(VI) phosphate complexes: their influence in uranium speciation in natural waters. *Geochimica et Cosmochimica Acta*, 56: 4135–4145.

Sato, T., Murakami, T., Yanase, N., Isobe, H., Payne, T. E. & Airey, P. L., 1997. Iron nodules scavenging uranium from groundwater. *Environmental Science and Technology*, 31: 2854–2858.

Sejkora, J., Babka, K. & Pavlíček, R., 2012. Saléeite from the uranium ore district Jáchymov (Czech Republic). *Bulletin mineralogicko-petrologického oddělení Národního muzea v Praze*, 20: 208–212. [In Czech, with English summary.]

Sejkora, J., Pauliš, P., Kopecký, S. & Kopecký, S., 2007. Saléeit z uranového rudního výskytu Heřmaničky u Votic. *Bulletin mineralogicko-petrologického oddělení Národního muzea v Praze*, 14-15: 114–115. [In Czech.]

Siuda, R., Domańska-Siuda, J. & Gołębiowska, B., 2010. Secondary uranium minerals from the Miedzianka–Ciechanowice deposit (Rudawy Janowickie Mts., Poland). *Mineralogia Special Papers*, 37: 107.

Siuda, R., Kruszewski, L. & Borzęcki, R., 2008. Uranospinite from abandoned Podgórze uranium mine in Kowary (the Karkonosze Mts. Poland). *Mineralogia Special Papers*, 32: 157.

Szałamacha, M., 1965. *Szczegółowa mapa geologiczna Sudetów, 1:25 000, arkusz Jelenia Góra Zachód.* Wydawnictwa Geologiczne, Warszawa. [In Polish.]

Szałamacha, M., 1972. *Szczegółowa mapa geologiczna Sudetów, 1:25 000, arkusz Piechowice.* Wydawnictwa Geologiczne, Warszawa. [In Polish.]

Thoreau, J. & a Vaes J. F., 1932. La saléeite, nouveau minéral uranifère. *Bulletin de la Société Belge de Géologie, de Paléontologie et d`Hydrologie*, 42: 96–100. [In French.]

Vochten, R. & van Springel, K., 1996. A natural ferrous substituted saléeite from Arcu su Linnarbau, Capoterra, Cagliari, Sardinia. *Mineralogical Magazine*, 60: 647–651.

Waite, T. D., Davis, J. A., Payne, T. E., Waychunas, G. A. & Xu, N., 1994. Uranium(VI) adsorption to ferrihydrite: application of a surface complexation model. *Geochimica et Cosmochimica Acta*, 58: 5465–5478.

Walczak, W., 1968. *Sudety*. Państwowe Wydawnictwa Naukowe, Warszawa, 383 pp. [In Polish.]

Yakubovich, O. V., Steele I. M., Atencio D., Menezes L. A. & Chukanov N. V., 2008. Crystal structure of the $(Mg,Fe)[UO_2(P,As)O_4]_2 \cdot 10H_2O$ solid solution – a novel mineral variety of saléeite. *Crystallography Reports*, 53: 764–770.